Counterintuitive Viscoelasticity of Supramolecular Polymer Networks Driven by Coassembly with Water Molecules

Emmanouil Vereroudakis, Nikolaos Burger, Laurent Bouteiller, Benoit Loppinet, E. Meijer, Dimitris Vlassopoulos, Nathan van Zee

Counterintuitive Viscoelasticity of Supramolecular Polymer Networks Driven by Co-assembly with Water Molecules

Emmanouil Vereroudakis,[1,2] Nikolaos A. Burger,[1,2] Laurent Bouteiller,[3] Benoit Loppinet,[1] E. W. Meijer,[4] Dimitris Vlassopoulos,[1,2] Nathan J. Van Zee[5*]

[1]*Foundation for Research & Technology Hellas (FORTH), Institute for Electronic Structure and Laser, Heraklion 70013, Greece;*

[2]*University of Crete, Department of Materials Science and Technology, Heraklion 70013, Greece*

[3]*Sorbonne Université, CNRS, IPCM, Equipe Chimie des Polymères, 75005 Paris, France*

[4]*Laboratory of Macromolecular and Organic Chemistry and Institute for Complex Molecular Systems (ICMS), Eindhoven University of Technology, 5600 MB Eindhoven, The Netherlands*

[5]*Chimie Moléculaire, Macromoléculaire, Matériaux, ESPCI Paris, Université PSL, CNRS, 75005 Paris, France*

TOC

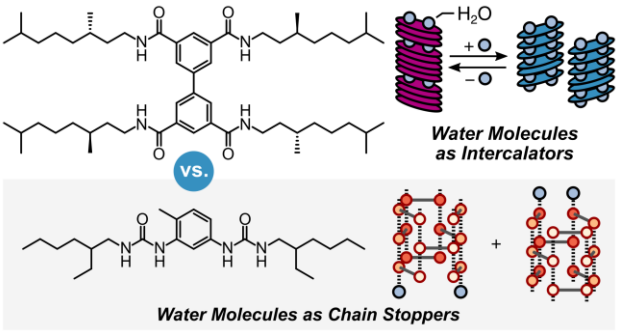

KEYWORDS: Supramolecular polymers, networks, co-assembly, rheology

ABSTRACT

Water molecules can play a striking role in dictating the structure of supramolecular polymer networks in apolar media, but the consequences on their viscoelasticity are not completely understood. Herein, we compare two synthetic supramolecular polymer networks based on hydrogen bonding motifs that co-assemble with water molecules in different ways. The first is a biphenyl tetracarboxamide (**BPTA**) that forms three different helical structures, two of which feature intercalated water molecules. The second is 2,4-bis(2-ethylhexylureido)toluene (**EHUT**), for which water molecules act as chain stoppers. Networks of each motif in n-dodecane were studied by light scattering, linear viscoelasticity, and passive microrheology while controlling the environmental conditions. At low temperatures in the presence of traces of water, both motifs form networks of dynamic, "living" supramolecular polymers. At high temperatures, in striking contrast to **EHUT** networks, **BPTA** networks behave like conventional covalent polymer chains. The counterintuitive behavior of **BPTA** networks is proposed to originate from enhanced dynamicity enabled by intercalated water molecules at low temperatures.

INTRODUCTION

Supramolecular polymer networks are a promising class of functional materials for applications that demand thermal reversibility and stimuli responsiveness. These properties are derived from the dynamic, non-covalent nature of the interactions that hold the monomer units together. Many reports have demonstrated that multicomponent co-assembly is a powerful approach for tuning and elaborating the rheology of such materials. A classic example is the use of chain stoppers to control the degree of polymerization of supramolecular polymers, which directly impacts their viscoelasticity.[1-4] In a more recent example, Aida and co-workers[5,6] created supramolecular materials that exhibit upper and lower critical solution temperatures by elegantly exploiting the competitive assembly between a supramolecular polymer and the clustering of alcohols in apolar solvents. Other recent studies on benzene tricarboxamides,[7,8] triarylamine tricarboxamides,[9] crown ether-based structures,[10,11] and bisureas[12-16] highlight how competitive

non-covalent interactions can be harnessed to create supramolecular networks and gels with unique rheological properties in organic solvents or aqueous media.[17]

An intriguing facet of this research concerns the role of minute amounts of water in dictating the structure and properties of self-assemblies in apolar media.[18,19] Contrary to simple aliphatic alcohols that tend to form clusters in such media,[5] water dissolved in alkane solvents exists in the molecularly dissolved state, even at saturation.[20,21] Thus, at sufficiently low temperature, there is an enthalpic driving force for water to interact with co-dissolved substrates that can form hydrogen bonds. For supramolecular polymer networks formed in oils, the nature of this interaction—along with its effect on material properties—depends on the chemical structure of the supramolecular monomer. Thus far, these interactions have only been described empirically; concrete design principles for specific water-based interactions remain to be established. Such understanding could have important implications for the development of supramolecular organogels, which have garnered interest in the fields of coatings, multi-functional sorbents, electronics, and drug delivery.[22]

In this context, the co-assembly of the chiral biphenyl tetracarboxamide **BPTA** (Figure 1a) with water molecules has proven to be a fascinating model system.[23-25] **BPTA** assembles at micromolar concentrations in methylcyclohexane (MCH) to form helical one-dimensional fibers assigned as state **A** (Figure 1b), which is distinguished by a positive Cotton effect at 258 nm by circular dichroism (CD) spectroscopy. When the temperature is sufficiently low and the concentration of co-dissolved water is sufficiently high, **A** undergoes sharp structural transitions to form two other kinds of fibers, states **B** and **C**, that have a positive Cotton effect at 250 nm and a negative Cotton effect at 238 nm, respectively. Spectroscopic and calorimetric experiments revealed that **B** and **C** are co-assemblies between **BPTA** and water molecules. Using a thermodynamic mass-balance model, we estimated that **B** and **C** contain 0.5 and 2.0 water molecules per **BPTA** molecule, respectively. Although the molecular structures of these assemblies remain unknown, FTIR spectroscopic measurements suggest that water molecules act as structural units between assembled **BPTA** monomers in states **B** and **C**, as schematically depicted in Figure 1b. Molecular models based on

density functional theory calculations confirm that clusters of water between assembled **BPTA** monomers are stable structures.

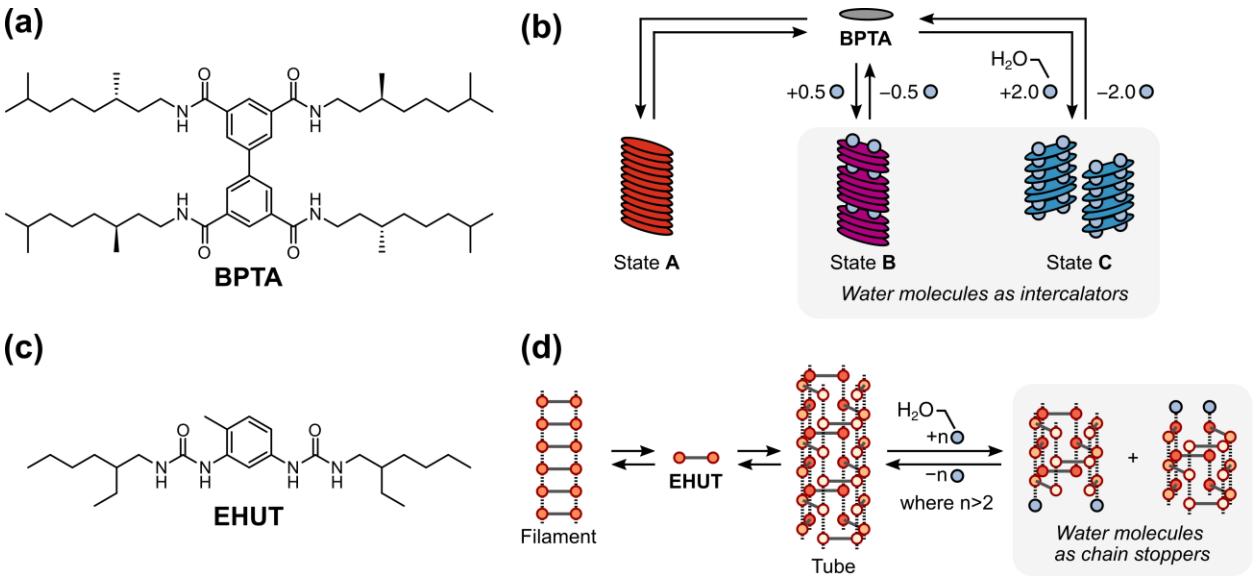

Figure 1. (a) Chemical structure of the biphenyl tetracarboxamide **BPTA**. (b) Schematic mechanism for the supramolecular co-assembly of **BPTA** with water to give states **A**, **B**, and **C**. The cartoons are qualitative representations of each state, and the stoichiometry was previously determined on the basis of a mass-balance model.[23] (c) Chemical structure of the bisurea **EHUT**. (d) Schematic mechanism for the supramolecular assembly of **EHUT** to give filaments (left) and tubes (center).[26-29]

Taken altogether, the water molecules are proposed to act as intercalators[30] in this system, with **BPTA** concentration, temperature, and water content acting as complementary parameters for controlling the helical state. Although the first studies were focused on understanding the co-assembly mechanism and the helical structure,[23,24] some key observations piqued our interest with respect to the viscoelasticity of these materials. For example, we noticed that after gently warming millimolar samples of **BPTA** in MCH, the solutions became noticeably less viscous upon reaching room temperature.

We were thus motivated to further explore the linear viscoelasticity (LVE) of **BPTA** networks. To bring greater perspective to this study, we sought to compare their LVE to that of another supramolecular polymer

network based on a different hydrogen-bonding motif that also co-assembles with water molecules in apolar media. Only a few relevant examples of have been reported, and the LVE of most of these systems is not yet well understood.[18,19] A notable exception, however, is supramolecular polymer networks based on the bisurea 2,4-bis(2-ethylhexylureido)toluene (**EHUT**, Figure 1c).[4,12,15,16,29,31-35] The phase diagrams for **EHUT** networks have been determined as a function of temperature, **EHUT** concentration, and pressure, revealing that **EHUT** assembles into either filaments or tubes depending on the conditions (e.g., low temperature, high concentration, and high pressure favor the formation of tubes). Networks prepared from **EHUT** tubes are thermodynamically stable and can be well-described by the model of Cates for "living" supramolecular polymers (vide infra).[33,36] The LVE of **EHUT** networks was studied by measurements within a humidity-controlled sample environment[29] and was found to depend on water content. To rationalize these findings, it was proposed that water molecules act as chain stoppers (Figures 1d, S1, and S2; see the Supporting Information for further discussion).[26-28] The competitive association of water presumably takes place at the ends of the fibers and leads to a reduction of the average length, but it does not appear to alter the packing of the **EHUT** monomers throughout the fibers.[29]

In the case of both **BPTA** and **EHUT** networks, water molecules compete with the homopolymerization of each respective monomer motif, but the outcomes in terms of polymer structure are strikingly different. We aimed to uncover how the different structural roles of water molecules impact the LVE of each respective supramolecular polymer network under different environmental conditions. Herein, we compared and contrasted the **BPTA** and **EHUT** systems based on a variety of techniques, including light scattering, conventional linear rheometry (small amplitude oscillatory shear, SAOS), and passive microrheology. All of these experiments were performed while carefully controlling the environmental conditions. We found that **BPTA** networks exhibit a striking evolution in the values of the viscoelastic moduli in response to temperature. At 35 °C, **BPTA** materials in state **A** behave as a network of “non-living” polymer chains made up of static, non-dynamic bonds. Counterintuitively, decreasing the temperature to access states **B** and **C** resulted in a speeding-up or slowing-down of the material’s relaxation dynamics depending on the water content; in both states, the material behaves like a network of “living”

supramolecular polymers held together by dynamic bonds, which is the same behavior observed for **EHUT** polymer networks. These trends were established with complementary experiments with varying relative humidity. We propose that the counterintuitive behavior of **BPTA** networks is attributable to enhanced dynamicity induced by the intercalated water molecules.

EXPERIMENTAL SECTION

Materials. $N^3,N^{3\prime},N^5,N^{5\prime}$-tetrakis((*S*)-3,7-dimethyloctyl)-[1,1'-biphenyl]-3,3',5,5'-tetracarboxamide (**BPTA**)[23] and 2,4-bis(2-ethylhexylureido)toluene (**EHUT**)[26] were prepared as previously reported. n-Dodecane (>99%) was either purchased from Sigma-Aldrich or Alfa Aesar and used as-received (i.e., each stock contained dissolved water that was absorbed from the ambient atmosphere). Sodium chloride (>99%), lithium chloride (>99%), and phosphorus pentoxide (>98%) were purchased from Sigma-Aldrich and used as-received.

Circular dichroism (CD) spectroscopy. Experiments were performed using a Jasco J-815 spectrometer equipped with a Jasco MPTC-513 multi-cell sample holder and temperature controller. The sample chamber was purged with nitrogen at a flow rate of 20 L/min. A quartz cuvette (Hellma Analytics) with a path length of 10 mm and a cap with a Teflon-coated septum was used.

Rheometry. Experiments were performed with an Anton-Paar (Austria) Physica MCR-501 rheometer equipped with a Peltier unit for temperature control (±0.1°C), which also constitutes the bottom plate, and a top cone geometry. All metallic components were made of stainless steel. Four different cones were used with a diameter (angle) of 8 mm (α=1°), 12.5 mm (α=1°), 25 mm (α=2°) and 50 mm (α=2°). The choice of dimensions was made based on the torque signal as needed. For samples with concentration below 5 g/L, a stainless steel Couette geometry (bob diameter=16.5 mm, cup diameter=17.0 mm, bob length=13.0 mm) was mounted on a strain controlled ARES 100 FRTN1 rheometer (TA, USA). The temperature was controlled with a Peltier unit. All measurements were performed at atmospheric pressure.

Samples were loaded at the desired temperature and immediately isolated from the ambient atmosphere with the humidity chamber.[29,37] After loading and equilibration, a rheological "rejuvenation" test was performed to erase the history of the sample due to preparation and loading on the measuring stage. The rejuvenation protocol consisted of a dynamic time sweep test at a fixed nonlinear strain, typically 700%, and fixed oscillatory frequency (1 rad/s) for a given time until full liquid-like behavior of the system was reached (typically 300 s).

Afterwards, the aging kinetics was followed with consecutive dynamic frequency sweep tests, and measurements were performed after the sample had reached its mechanical steady-state. The linear viscoelastic regime was determined by dynamic strain sweep tests and is defined as the regime in which the dynamic moduli are independent of the applied strain amplitude. Creep measurements (step stress) were performed to study the higher concentration samples. When the applied stress was within the linear viscoelastic regime, the creep response (compliance) was converted into dynamic moduli through the relaxation/retardation spectra.[38] Here, the creep compliance $J(t)$ was converted to $G'(\omega)$ and $G''(\omega)$ by means of the NLReg software based on a generalization of the Tikhonov regularization method.[39] This approach allowed extending the LVE spectrum determined by SAOS measurements.

Static light scattering (SLS). Measurements were performed at different temperatures in the range of 15 to 35 °C and at scattering angles (θ) ranging from 15° to 150° using an ALV-5000 (Germany) goniometer setup with a cw Nd:YAg laser (λ_0 = 532 nm). The temperature was controlled with a recirculating water/ethylene glycol bath. The samples were equilibrated for 60 min upon each change in temperature. Each observation angle corresponds to a scattering wave-vector $q = \frac{4\pi n_s}{\lambda_0} \sin\left(\frac{\theta}{2}\right)$, where n_s is the refractive index of the solvent.

Dynamic light scattering (DLS) and passive microrheology. Measurements were conducted using a homemade setup that has been reported previously.[15,35,40,41] A cw Nd:Yag laser at 532nm was used, and

measurements were made at a fixed scattering angle of 90°. A mono-mode optical fiber was used to transfer the scattered light into a photomultiplier tube.

For microrheology, polymethylmethacrylate (PMMA) particle probes were added at a volume fraction of about 0.01%. The particles were chemically grafted with poly(hydroxystearic acid) chains (with a length of about 10 nm) to ensure proper dispersion of the probes, and they had a hydrodynamic radius of 130 nm with a polydispersity on the order of 10%.[42] Under these conditions, at 25 °C the PMMA probes and the solvent have refractive index values of 1.49 and 1.42, respectively.[43] For high concentration samples (c > 8 g/L) and high temperatures (about 180 °C), the experiments were performed with another homemade setup that has been reported previously.[15] The scattering intensity was collected by means of an optical mono-mode fiber via a respective sample window at 90° scattering angle.

In one experiment, a CCD camera was used to acquire multi-speckle patterns in a series of images during a temperature ramp from 180 °C to room temperature. Variations in the resulting scattering intensity were interpreted as signatures of the different states of the material.

Sample preparation. For CD spectroscopy and SLS experiments, samples of **BPTA** (up to 0.1 g/L in n-dodecane) were prepared by heating, vortexing, and sonicating for approximately 1 h, which was followed by mixing overnight at 20 °C using a sample shaker.

For SAOS measurements, samples of **BPTA** (from 1.8 to 90 g/L in n-dodecane) were prepared by heating, vortexing, and sonicating every hour for 45 min for three consecutive days until they became homogeneous to the eye. This process was followed by an equilibration period of ten days at 20 °C. The equilibration period was determined on the basis of control experiments that consisted of following the heating/vortexing/sonicating protocol and subsequent measurement of the mechanical properties and aging of the material at well-controlled conditions. Samples of **EHUT** were prepared as described previously,[16,29,35] which consisted of adding the desired quantity of **EHUT** powder (stored under ambient conditions) to n-dodecane and then stirring at 80 °C for 48 h.

For DLS and passive microrheology, samples of **BPTA** (from 1.0 to 8.0 g/L in n-dodecane) were prepared in the same way as described above for SAOS experiments. Before commencing each experiment (or set of experiments), the sample was allowed to equilibrate in the sample tube overnight at 20 °C. Samples of **EHUT** were prepared in the same way as described above for the SAOS measurements.

THEORETICAL BACKGROUND

Given that the linear viscoelastic properties of **EHUT** networks have been extensively discussed in terms of the model of Cates for "living" polymers,[36,44] it is useful to briefly review the key elements of this framework to facilitate the interpretation of the results of the **BPTA** system. In general, supramolecular monomers can assemble into long fibers that interact with each other, resulting in a three-dimensional network.[45,46] "Living" supramolecular polymers are defined as being able to undergo reversible chain scission and recombination reactions to relax an imposed stress, which is similar to the behavior of wormlike surfactant micelles.[47] Thus, both monomer-monomer and entanglement-like fiber-fiber interactions dictate the relaxation dynamics of the system. These two processes correspond to two timescales: the breaking time (τ_b) and the reptation time (τ_r), respectively. In the fast-breaking limit (i.e., $\tau_b < \tau_r$), the terminal relaxation time is defined as $\tau_t = (\tau_b \tau_r)^{0.5}$, and the storage and loss moduli follow a single exponential Maxwell behavior at low frequencies (terminal regime). Assuming that the average micellar length (L) scales with the breaking time as $\tau_b \sim L^{-1}$ and that L scales with concentration (c) as $L \sim c^{0.5}$, the terminal relaxation time scales with concentration as $\tau_t \sim c^{1.25}$. As for semi-dilute polymer solutions, the plateau modulus (G_0) is proposed to scale with c as $G_0 \sim c^{2.25}$.[48]

In contrast, for static, “non-living” supramolecular polymers in the non-breaking limit (i.e., $\tau_b >> \tau_r$), the chain scission and recombination processes are too slow to contribute to stress relaxation, which is similar for covalent macromolecular analogues. The terminal relaxation time is thus simply equal to the reptation time. Such systems are expected to follow scaling laws predicted within the reptation model for semi-dilute polymer solutions.[48] For the plateau modulus and the terminal relaxation time, these relationships are $G_0 \sim c^{2.25}$ and $\tau_t = \tau_r \sim c^{2.25}$, respectively. It should be noted that the above model does not consider non-reptative

mechanisms (e.g., contour length fluctuations and constraint release). Alternative approaches to constitutive modeling, also accounting for nonlinear effects, and a slip-link simulation model were recently presented.[44,49-52] However, we note that the nonlinear response is not addressed in this work.

RESULTS AND DISCUSSION

Self-assembly and aging effects. All **BPTA** and **EHUT** networks were prepared in n-dodecane, an alkane with a high boiling point (216 °C) and a melting transition below room temperature (−10 °C),[53] to minimize evaporation during the experiments. The assembly of **EHUT** networks in n-dodecane has already been studied,[15,16,29,34] but all previously reported experiments with **BPTA** were performed in MCH or heptane.[23-25]. As discussed in the Supporting Information (Figures S3), CD spectroscopy measurements confirmed that **BPTA** assembles in n-dodecane in essentially the same way as reported previously. In particular, the material was found to be in states **A**, **B**, and **C** (Figure 1b) at 35, 25, and 15 ° C, respectively, under ambient humidity.

To begin to explore how the co-assembly of **BPTA** with water impacts the higher order structure of the aggregates, static light scattering (SLS) experiments were performed on samples under relatively dilute conditions (0.09 g/L in n-dodecane). In Figure 2, the excess scattering ratio R_{vv} is plotted as a function of wave-vector q at 15, 25, and 35 °C, corresponding to the formation **C**, **B**, and **A**, respectively. A change in the scaling of R_{vv} is observed, going from q^{-2} at 15 °C for **C** to q^{-1} at 25 and 35 °C for **B** and **A**, respectively. The leveling-off of the intensity at lower q values at 15 °C indicates that the overall size of **C** was nearly captured in the experiment; this is not the case for **A** and **B**. The transitions between these different states at higher concentrations of **BPTA** (1.0 to 8.0 g/L in n-dodecane) were evidenced by dynamic light scattering and microrheology experiments as discussed in the Supporting Information (Figures S4–S6).

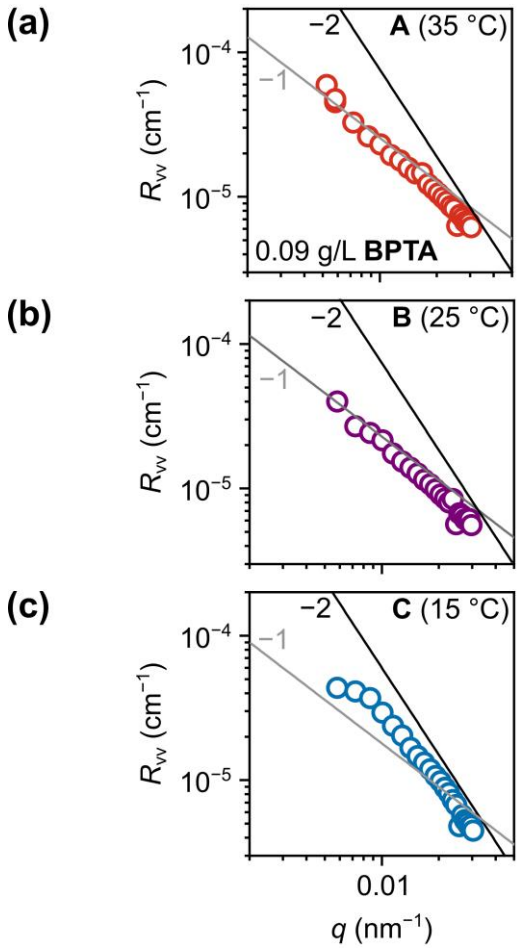

Figure 2. Excess scattering ratio as a function of wave-vector of **BPTA** (0.09 g/L in as-received n-dodcane) at (a) 35, (b) 25, and (c) 15 °C. Lines with slopes of −1 (grey) and −2 (black) reflect the behavior of rod-like and flexible chains, respectively.

Careful control of the sample environment was required for exploring the viscoelasticity of these materials. Building upon previous work,[29] we recently designed an improved chamber to isolate the sample from the ambient environment during linear SAOS measurements, allowing for the rigorous control of temperature and humidity while suppressing unwanted evaporation of the sample (Figure S7a).[37] The relative humidity (*RH*) could be easily controlled by loading desiccants or salt solutions into compartments within the chamber; target *RH* values were rapidly reached and remained stable for at least 30 h (Figure S7b).

Even in the absence of an external stimulus, many supramolecular polymers are metastable structures that build up over time,[54-56] resembling the assembly of proteins in biological systems (e.g., gelatin and actin filaments). Despite the stability of the environmental conditions, we found that **BPTA** networks were subject to aging over hours and days. For example, the evolution of the spectra of a 45 g/L **BPTA** sample that was loaded into the environmental control chamber of the rheometer is depicted in Figure 3. In this experiment, the **BPTA** sample had been equilibrated at 20 °C for several days before being loaded into the chamber that was pre-heated to 35 °C with ambient *RH*. Over the course of 14 h, the plateau modulus increased by a factor of 1.5, while the crossover frequency of *G*' and *G*" shifted by over a decade toward lower frequency. The shift in the crossover frequency became less pronounced over time, suggesting that the system approached a steady state.

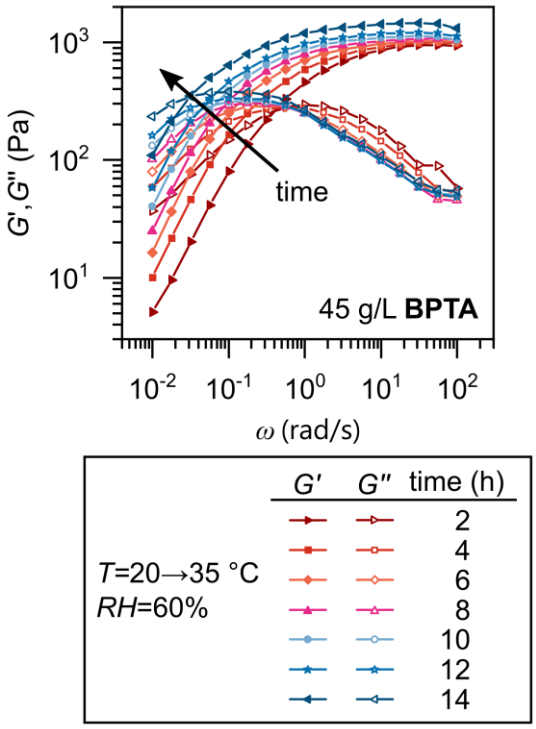

Figure 3. Evolution of rheological spectra of a 45 g/L **BPTA** sample upon loading on the rheometer. The sample had been stored at 20 °C before being loaded into the chamber that had been pre-heated to 35 °C.

Although the origin of this aging remains unclear, an important factor for samples that have a high loading of **BPTA** is the wide fluctuations in water content required to effect each structural transition. For example, taking into consideration the stoichiometry of water in states **B** and **C** (i.e., 0.5 and 2.0 molecules of water per molecule of **BPTA**, respectively, see Figure 1b),[23,24] a 45 g/L (51 mM) sample of **BPTA** requires water concentrations of 25 and 101 mM to form states **B** and **C**, respectively. These values are in excess of the concentration of water in saturated n-dodecane, which is only 2.7 mM.[57] Thus, at sufficiently low temperature, **BPTA** networks must absorb a significant amount of water from the atmosphere to access states **B** and **C**.

We hypothesized that this process is slow compared to the timescale of the SAOS measurements, given the relatively limited surface area of the sample that is exposed to atmosphere (Figure S7a) along with the retarded mobility of water molecules in the presence of hydrogen bond-based aggregates.[58] These considerations are unlikely to be important in the case of **EHUT** because the stoichiometry of the interaction with water as chain stoppers is comparatively far less than that determined for states **B** and **C** in the **BPTA** system. As previously discussed,[29] if we assume that at least two molecules of water are required to end-cap a chain and apply the chain stopper model,[26] the observed decrease in the relaxation time for **EHUT** networks in n-dodecane (loading of 5 g/L or 12 mM) is calculated to require 10 ppm (0.6 mM) of co-dissolved water.

To compare the aging behavior of **BPTA** and **EHUT** networks in the absence of water effects, we sought to perform rheological experiments at elevated temperatures. For example, in the case of **BPTA** networks, the measurements should be conducted well above the expected transition temperatures for **A**→**B**. Conventional rheometry was not well suited for these experiments due to issues of evaporation at high temperature. Passive microrheology was employed instead because a closed sample environment (with a relatively small headspace) could be used. The **BPTA** network (2.1 g/L sample prepared under ambient humidity) was thus heated up to 160 and then cooled to 75 °C; this temperature was maintained while measurements were performed over time (frequency sweep and creep compliance data presented in Figures 4a and S8, respectively). Going from 0.5 to 22 h, a subtle shift toward slower kinetics was observed. After

72 h, the dynamics became more prominently retarded, revealing the propensity of **BPTA** fibers to slowly evolve in structure even in the absence of strong interactions with water. Conversely, **EHUT** networks (Figure 4b) at 81 °C appeared to be under thermodynamic equilibrium because they do not exhibit any evolution in viscoelasticity with time, consistent with previous studies.[15,29,33]

Thus, before all SAOS measurements of **BPTA** networks discussed below, samples were equilibrated under the desired environmental conditions. Frequency sweep measurements were periodically performed during the equilibration period until a nearly steady state was achieved (typically 5–30 h). No such protocol was necessary for the **EHUT** networks.

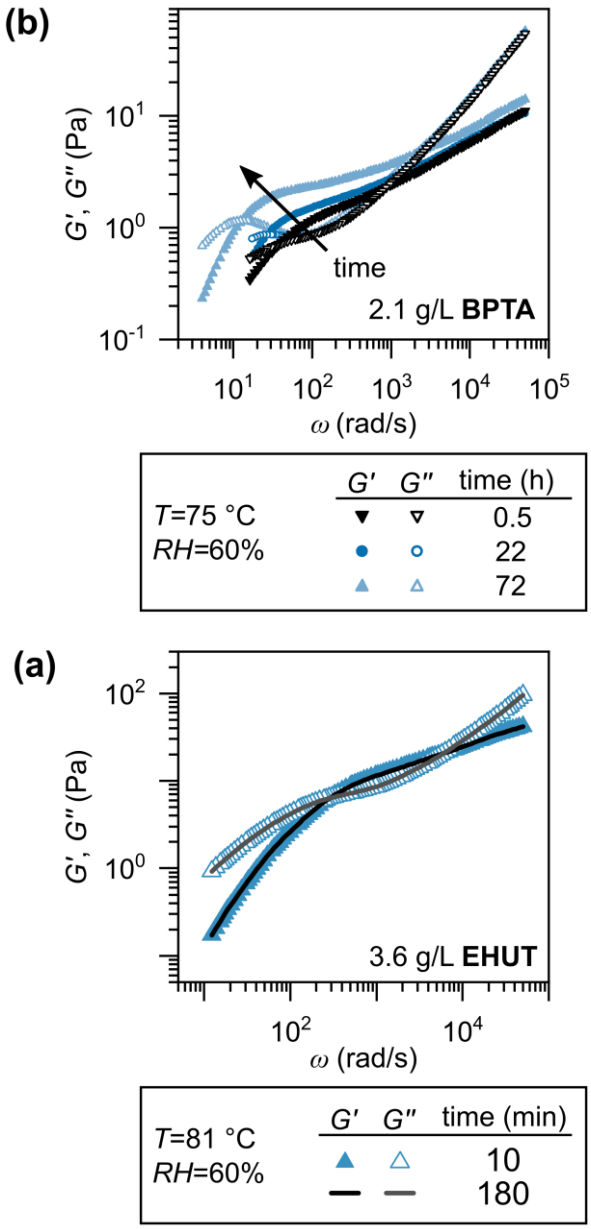

Figure 4. Passive microrheological aging experiments conducted on (a) a **BPTA** network (2.1 g/L) at 75 °C and (b) an **EHUT** network (3.6 g/L) at 81 °C.

Modulating viscoelasticity by altering the temperature. We thus explored the LVE of **BPTA** and **EHUT** networks as a function of temperature and monomer concentration while maintaining constant *RH*. A series of **BPTA** solutions ranging from 1.8 to 90 g/L were prepared and measured at 35, 25, and 15 °C (*RH*=60%) to study states **A**, **B**, and **C**, respectively. These experiments relied on the fact that the transitions **A**→**B** and

B→C (along with the corresponding reverse reactions) are independent of the **BPTA** concentration.[23] Representative data for **EHUT** networks at similar concentrations and temperatures have been previously reported[29] and are presented here for comparison. The **EHUT** samples ranged from 2 to 12 g/L (*RH*=40%) and were measured at 25 °C. The experimental conditions for the **EHUT** materials were entirely within the tube region of its phase diagram.[12-15]

The SAOS results for **BPTA** samples at 1.8, 9.0, and 90 g/L are presented in Figure 5, and the complete set of data is provided in Figure S9. Across all temperatures, the dynamics of the **BPTA** networks become slower as the concentration of **BPTA** increases. For example, in state **A** at 35 °C, the sample is a viscoelastic liquid at 1.8 g/L because the crossover frequency (ω_c) of the storage (G') and loss (G'') moduli and terminal regime are accessible, while the plateau modulus is within the limits of the experimental window of the rheometer. As the **BPTA** concentration increases, ω_c shifts to lower frequencies, and the sample becomes an entangled network at 90 g/L. In contrast, in state **B** at 25 °C, the sample is an entangled network at all concentrations examined.[59-61] In state **C** at 15 °C, the system remains a relatively weak viscoelastic liquid across all temperatures and concentrations.

We attempted to fit each of the viscoelastic spectra in the plateau to terminal regime to a single Maxwell mode (representative fits are indicated by thin colored lines in Figure 5), which is a feature expected for living supramolecular polymers in the fast-breaking limit as discussed above.[7,9,36,47,62] At low frequencies, the data are in good agreement at 15 °C between 4.5–45 g/L and at 25 °C for concentrations up to 45 g/L. At 35 °C, the terminal relaxation of the system at all concentrations is much broader compared to that observed at 15 and 25 °C, as revealed by the discrepancy between the data and the Maxwell model predictions. At 90 g/L, there is deviation from simple Maxwell behavior at all temperatures, suggesting that the interactions in the system become more complex at higher concentrations.[36,63]

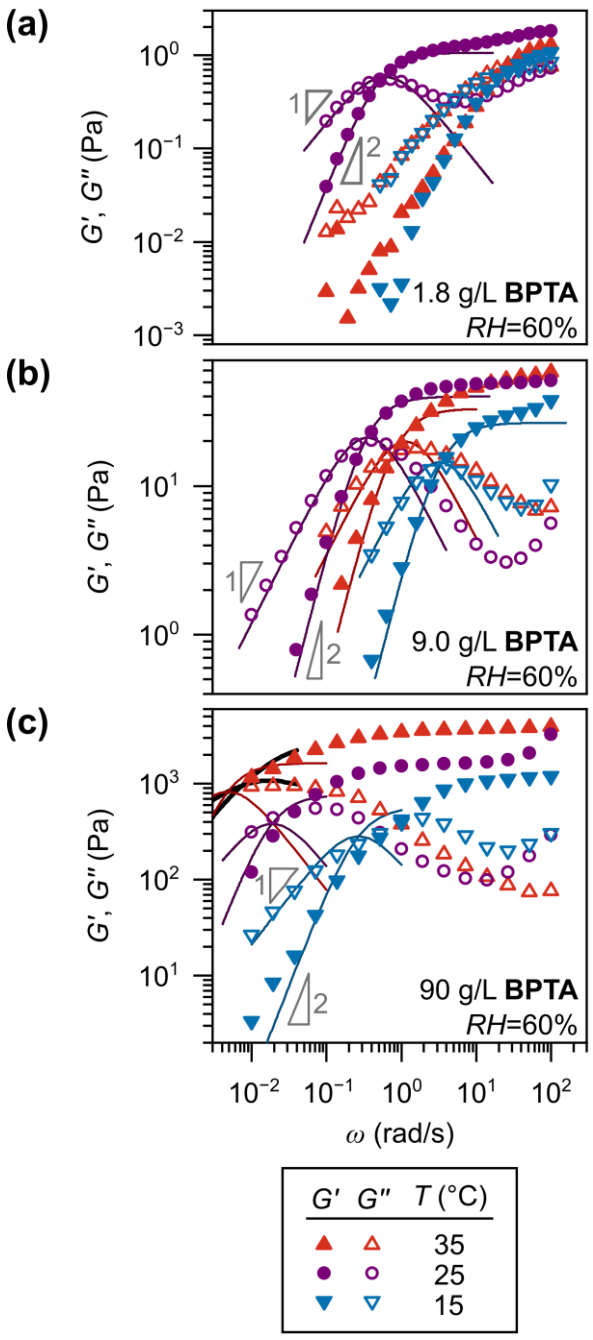

Figure 5. Linear viscoelastic spectra acquired by SAOS measurements of **BPTA** in n-dodecane at (a) 1.8, (b) 9.0, and (c) 90 g/L. The relative humidity (*RH*) was maintained at 60% for all measurements. The thin colored lines in each pot represent the best fit of each respective set of data with a single Maxwell mode. The thick black lines in (c) represent converted creep compliance data. Scaling of the storage and loss

moduli in the terminal regime are included in grey. Note the deviations of the Maxwell mode from the data with increasing concentration and frequency above the terminal crossover.

Further insight is gained by comparing the scaling of G_0 (defined as the value of *G'* at the frequency of the minimum of *G"*) and τ_t (defined as the inverse frequency at the crossover of *G'* and *G"*, $1/\omega_c$) as a function of concentration. In Figure 6a, G_0 is plotted as a function of c for all temperatures in a double logarithmic representation. As a comparison, a data set for **EHUT** networks is included based on literature values.[29] For **BPTA** networks in states **A**, **B**, and **C**, as well as the **EHUT** system, the plateau modulus scales nearly as $G_0 \sim c^{2.25}$, which is predicted by Cates and typical of polymeric networks.[48]

With respect to the scaling of the terminal relaxation time with concentration, the data are represented in two different ways to facilitate the discussion. In Figure 6b, the scaling of τ_t with concentration is presented as a log-log plot. In Figure 6c and d, the data are represented as assembly landscapes[64] of temperature versus concentration for the **BPTA** and **EHUT** networks, respectively; each data point is colored based on the value of τ_t. The dashed lines indicate barriers between the indicated supramolecular structures. For the **BPTA** networks, the positioning of these barriers is proposed based on the data presented in the present manuscript as well as the previous mechanistic study,[23,24] while for the **EHUT** networks the barriers are represented according to a previously-reported phase diagram.[15]

We first note that **BPTA** networks in states **B** and **C**, along with the **EHUT** networks, exhibit a scaling of $\tau_t \sim c^{0.77}$, which does not agree with the predicted scaling of Cates.[36,47,62] This discrepancy is likely attributable to the experimental scaling of average micellar length with concentration being different from what is assumed in the model (i.e., $L \sim c^{0.5}$),[29,65] as already discussed in the literature;[66,67] it may also reflect a different breaking/recombination mechanism.[44,63] For the **BPTA** networks in state **A**, a scaling of $\tau_t \sim c^{2.25}$ is observed, suggesting that the material is not in the fast-breaking limit. This different scaling is consistent with the deviation from single Maxwell mode behavior noted in the discussion of Figure 5. The dynamics of state **A** exhibit the concentration scaling of an entangled solution of "non-living" flexible polymers in a theta solvent.[48] In comparison with other supramolecular systems, such "non-living" behavior has been

reported for wormlike micelles with large breaking times that are comparable or larger than the reptation time.[47,68]

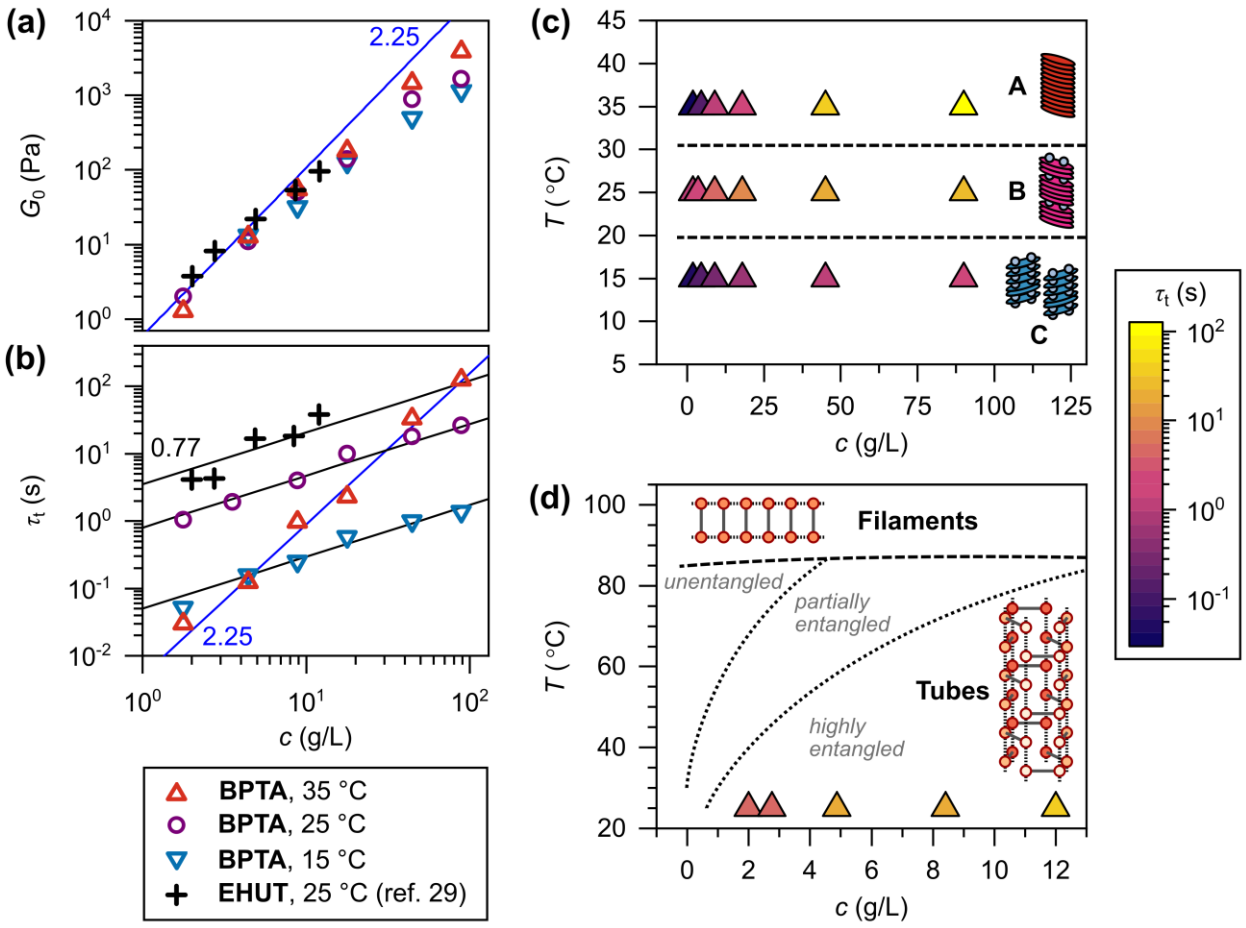

Figure 6. Scaling of the (a) plateau modulus, G_0, with concentration, c, and (b) scaling of the terminal relaxation time, τ_t, with c. The blue lines have a slope of 2.25 and the black lines have a slope of 0.77. Assembly landscapes[64] of temperature versus concentration for (c) **BPTA** networks and (d) **EHUT** networks.[15] The data points are color-coded based on their respective τ_t values according to the gradient color scale. The dashed lines indicate transitions between supramolecular structures. In (a), (b), and (d), the data for the **EHUT** networks were taken from the literature.[29]

The discrepancy in the terminal relaxation time scaling between state **A** and states **B** and **C** correlates with the counterintuitive viscoelastic profiles for **BPTA** materials as they are cooled from 35 to 15 °C at ambient *RH* (Figure 6b). For example, at high concentration (i.e., above 30 g/L **BPTA**), the network exhibits faster relaxation dynamics at 25 and 15 °C than at 35 °C. At intermediate concentration (i.e., between 5 and 30 g/L **BPTA**), the relaxation dynamics fluctuate, first becoming slower upon reaching 25 °C and then becoming faster at 15 °C. At low concentration (i.e., below 5 g/L **BPTA**), the relaxation dynamics become slower upon cooling from 35 °C to 25 °C but then slower upon further cooling to 15 °C. This behavior is in contrast to that of **EHUT** networks and to living supramolecular polymers in general. These different scaling regimes at each temperature coincide with the different states of the **BPTA** fibers: state **A** is effectively a homopolymer of **BPTA** monomers, while states **B** and **C** contain intercalated water molecules. In the subsequent sections, we aim to substantiate that intercalated water is indeed responsible for the unusual rheology of **BTPA** networks.

Relative humidity as a complementary means to modulate viscoelasticity. We previously established that the transitions **A**→**B** and **B**→**C** can be realized under dilute conditions at constant temperature by increasing the water content (and that the corresponding reverse reactions can be effected by decreasing the water content).[24] Temperature and water content are complementary factors for controlling the state of the **BPTA** fibers. We sought to apply the same experimental protocol to SAOS measurements by taking advantage of our ability to control the humidity and temperature of the environment. The conditions were selected to highlight the impact of the various **BPTA** states on the viscoelasticity of the material. Comparable conditions were also applied to **EHUT** networks by varying humidity and temperature in tandem.

A series of SAOS experiments were thus performed on **BPTA** (90 g/L, 25 °C) and **EHUT** (8.0 g/L, 20 °C) networks at constant concentration and temperature while the *RH* was varied from 5 to 100%. The concentrations of the **BPTA** and **EHUT** monomers were chosen so that the relaxation times of the resulting networks were within a similar range. In the case of **BPTA** networks (Figure 7a), as the *RH* is increased,

the crossover frequency increases by over two orders of magnitude, while the plateau modulus G_0 decreases by a factor of 3.5. For **EHUT** networks (Figure 7b), as the *RH* is increased from 5 to 100%, the crossover frequency of **EHUT** networks increases by less than a decade, which is consistent with the results of our previous study.[29] The plateau modulus decreases by a factor of about 1.6, and the overall shape of the spectra is independent of the *RH*.

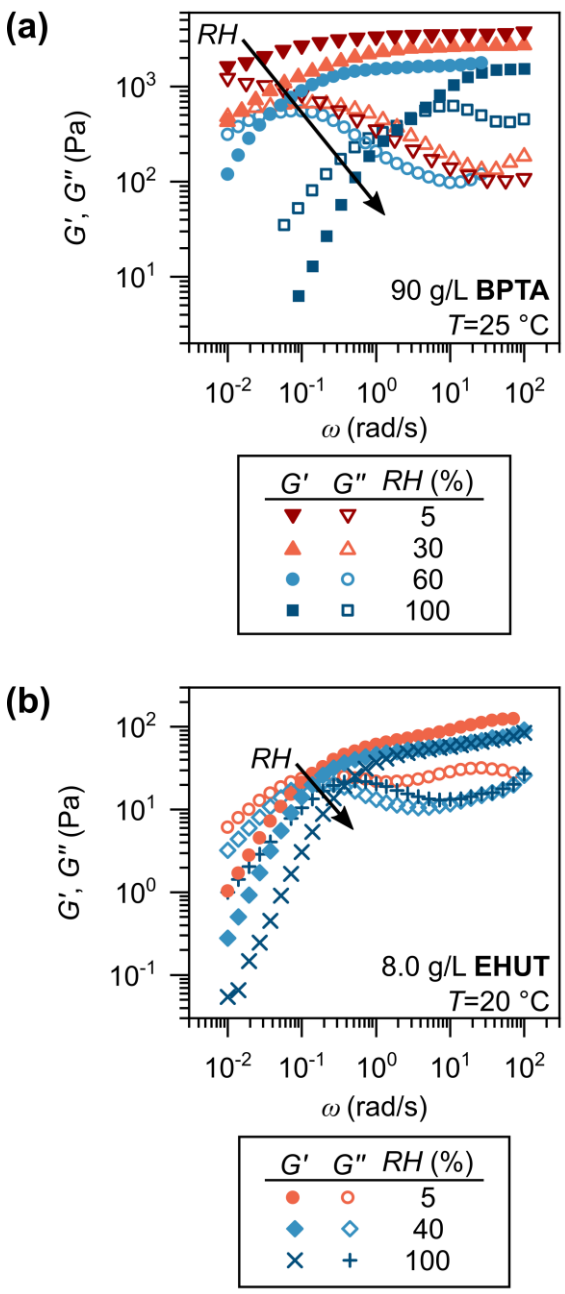

Figure 7. (a) Linear viscoelastic spectra of **BPTA** (90 g/L in n-dodecane) at 25 °C with varying *RH*. (b) Representative data for **EHUT** (8.0 g/L in n-dodecane) acquired at 20 °C and atmospheric pressure with varying *RH*.

Additional experiments were performed on **BPTA** (90 g/L) and **EHUT** (8.0 g/L) networks in which both the temperature and the *RH* were varied to assess the scaling of τ_t. Similar to above, these data are

represented in two different ways. In Figure 8a, the values of τ_t at different levels of *RH* are plotted as a function of temperature. In Figure 8b and c, these data are presented as temperature versus *RH* assembly landscapes for the **BPTA** and **EHUT** networks, respectively. The dashed lines in Figure 8b indicate transitions between supramolecular structures. The shapes of these boundaries are proposed based on previous mechanistic insights[23] and the presence of large step-changes between values of τ_t. In the case of **EHUT**, consistent with previous work,[29] no change in microstructure was detected as a function *RH* in the present study.

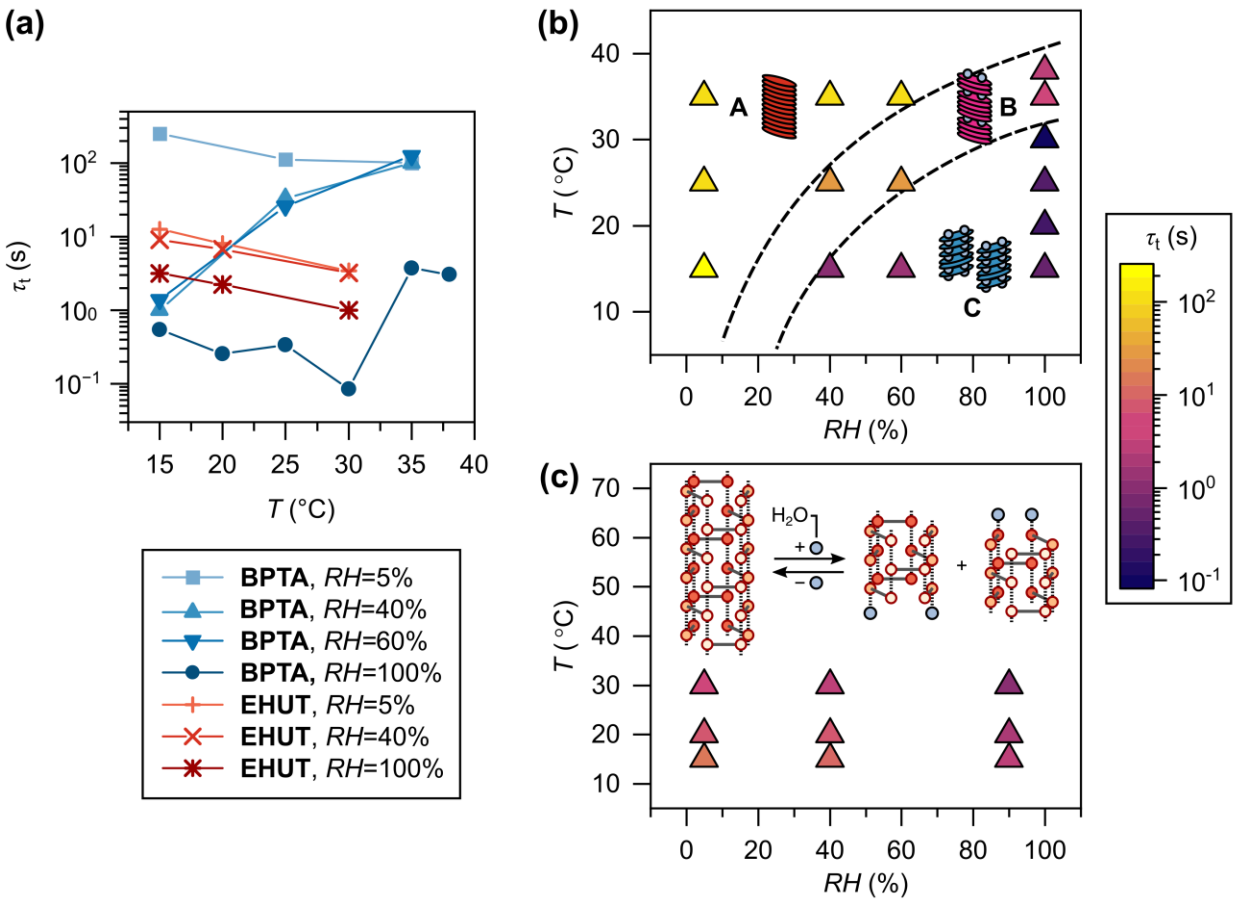

Figure 8. (a) Scaling of τ_t with temperature for **BPTA** (90 g/L in n-dodecane) and **EHUT** (8.0 g/L in n-dodecane) at different levels of *RH*. Assembly landscapes of temperature versus *RH* for (b) **BPTA** networks and (c) **EHUT** networks. The data points are color-coded based on their respective τ_t values according to the gradient color scale. The dashed lines indicate transitions between supramolecular structures.

For **EHUT**, τ_t gradually decreases with increasing temperature regardless of the *RH*. In contrast, for **BPTA**, τ_t exhibits a complex dependence and spans over two orders of magnitude depending on the conditions (i.e., *RH* and state of self-assembly). At 5% *RH*, **BPTA** networks exhibit τ_t values of 100 s at 35 °C to 250 s at 15 °C; these values are consistent with the dynamics of state **A** at 35 °C and 60% *RH* (Figures 6b and c). The formation of state **A** at low temperature and low water content is consistent with our previous studies.[23,24]

At *RH* values of 40 and 60%, τ_t drops approximately one decade between each temperature step going from 35 to 25 to 15 °C, consistent with the system being in states **A**, **B**, and **C**, respectively. This behavior is remarkable because the dynamics of the network become *faster* upon cooling, which is in stark contrast to the behavior of **EHUT** networks in particular and the expected behavior of conventional supramolecular networks in general. We believe that these results highlight the impact of water co-assembly on the dynamics of **BPTA**-based system.

At an *RH* of 100%, values of τ_t values remain at approximately 0.3 s until 35 °C, above which the dynamics significantly slow, with τ_t values reaching approximately 3 s. We interpret these results as corresponding to the formation of state **C** at low temperatures and reaching state **B** at the higher temperatures; at the saturation limit of water in the material, state **A** does not form at temperatures at least up to 38 °C. These results at 100% *RH* closely agree with the transition temperatures observed for **A**→**B** and **B**→**C** in a control experiment in which **BPTA** was assembled under dilute conditions over a droplet of water (Figure S10).

Finally, it is interesting to note the similarities between different viscoelastic spectra recorded for **BPTA** (90 g/L) by changing temperature and *RH* in tandem. For example, networks at 25 °C with *RH* values of 5 and 100% (Figure 7a) are very similar to those measured at 35 and 15 °C with an *RH* of 60%, respectively (Figure 5c). An explicit example is presented in Figure 9, where the viscoelastic spectra acquired at 35 and 15 °C at two different *RH* values are compared. At 35 °C, the system appears to be in state **A** at both 5 and

60% *RH* (dark red squares and orange crosses, respectively), as both feature a G_0 of approximately 4 kPa and a τ_r of over 100 s. At 15 °C with an *RH* value of 60%, the network is in state **C**, with a G_0 of 1.1 kPa and a τ_r of 1 s. Under dry conditions at 15 °C, G_0 reaches 3.6 kPa and τ_r decreases by over two orders of magnitude, consistent with the formation of state **A** under these conditions. These results confirm that the complementarity of temperature and water content for controlling the state of the **BPTA** fibers extends to the control of the viscoelasticity of the networks.

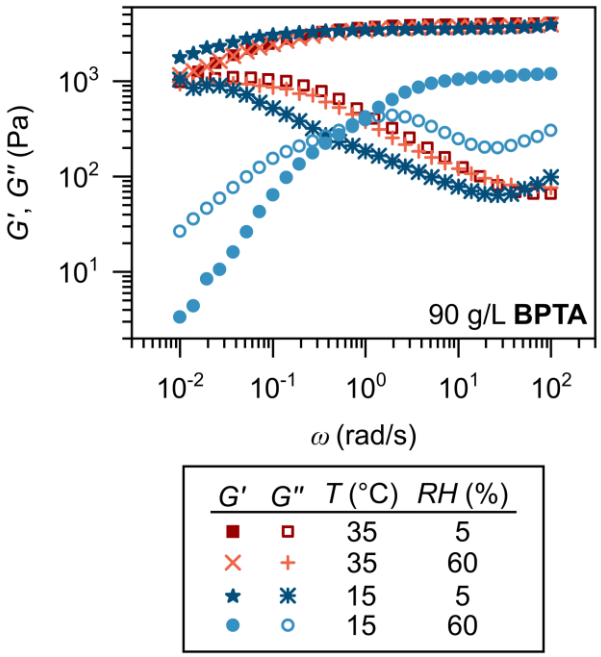

Figure 9. Comparison of the viscoelastic spectra of 90 g/L **BPTA** networks at 35 and 15 °C with either 5 or 60% *RH*.

CONCLUSIONS

BPTA and **EHUT** networks exhibit remarkably different linear viscoelastic properties in response to changes in temperature and relative humidity. A key finding is that **BPTA** networks exhibit complex relaxation dynamics. They behave as if they are made up of "non-living", conventional covalent polymer chains in state **A**, which is favored at relatively high temperature. Conversely, they behave like networks

of dynamic "living" supramolecular polymer chains in states **B** and **C**, which are favored to form at comparatively lower temperatures. We propose that this unusual behavior is due to enhanced dynamicity imparted by the intercalated water molecules present in states **B** and **C**. Experiments with varying relative humidity helped to establish that the intercalation of water molecules is the main driving force for this unusual evolution of dynamicity. In the case of **EHUT**, the binding of water also impacts relaxation dynamics but in a different way. Acting as chain stoppers, water molecules reduce the average chain length of the **EHUT** tubes, resulting in a decrease in the terminal relaxation time. Nevertheless, **EHUT** materials can be well-described as a network of "living" supramolecular polymers at both high and low relative humidity.

This study showcases the complex interplay between the chemical structure of the supramolecular monomer units, the structure of the supramolecular polymer, and the dynamics of the resulting networks. Moreover, these findings highlight the striking impact of water molecules on the structure and properties of supramolecular polymers in apolar media. We hope that this work will inspire further investigations of competitive interactions in supramolecular polymer networks to elegantly control their linear and non-linear rheological properties.

ASSOCIATED CONTENT

Sensitivity of filament-to-tube transition temperature to water content in **EHUT** organogels; supplementary experiments showing the assembly of **BPTA** in n-dodecane; humidity control for rheology experiments under ambient pressure; aging effects; supplementary rheological data; and CD spectroscopy characterization (Figures S1–S10).

AUTHOR INFORMATION

Corresponding Author

*Nathan J. Van Zee, nathan.van-zee@espci.psl.eu

Notes

The authors declare no competing financial interest.

ACKNOWLEDGMENTS

Fruitful discussions and preliminary experiments with M. F. J. Mabesoone (TU/e) are gratefully recognized. Enlightening discussions with J. D. Peterson (UCLA) are also gratefully acknowledged. We thank D. Parisi for technical assistance at the early stages of this work. Partial support has been received by the European Commission (Horizon2020-INFRAIA-2016-1, EUSMI grant no. 731019) and the Greek Secretariat for Research and Technology (INNOVATION program-AENAO).

REFERENCES

(1) Sijbesma, R. P.; Beijer, F. H.; Brunsveld, L.; Folmer, B. J.; Hirschberg, J. H.; Lange, R. F.; Lowe, J. K., Meijer, E. W. Reversible polymers formed from self-complementary monomers using quadruple hydrogen bonding. *Science* **1997**, *278*, 1601–1604.

(2) Folmer, B. J. B.; Cavini, E.; Sijbesma, R. P., Meijer, E. W. Photo-induced depolymerization of reversible supramolecular polymers. *Chem. Commun.* **1998**, 1847–1848.

(3) Michelsen, U., Hunter, C. A. Self-Assembled Porphyrin Polymers. *Angew. Chem. Int. Ed.* **2000**, *39*, 764–767.

(4) Knoben, W.; Besseling, N. A.; Bouteiller, L., Stuart, C. M. Dynamics of reversible supramolecular polymers: independent determination of the dependence of linear viscoelasticity on concentration and chain length by using chain stoppers. *Phys. Chem. Chem. Phys.* **2005**, *7*, 2390–2398.

(5) Venkata Rao, K.; Miyajima, D.; Nihonyanagi, A., Aida, T. Thermally bisignate supramolecular polymerization. *Nat. Chem.* **2017**, *9*, 1133–1139.

(6) Rao, K. V.; Mabesoone, M. F. J.; Miyajima, D.; Nihonyanagi, A.; Meijer, E. W., Aida, T. Distinct Pathways in "Thermally Bisignate Supramolecular Polymerization": Spectroscopic and Computational Studies. *J. Am. Chem. Soc.* **2020**, *142*, 598–605.

(7) Vereroudakis, E.; Bantawa, M.; Lafleur, R. P. M.; Parisi, D.; Matsumoto, N. M.; Peeters, J. W.; Del Gado, E.; Meijer, E. W., Vlassopoulos, D. Competitive Supramolecular Associations Mediate the Viscoelasticity of Binary Hydrogels. *ACS Cent. Sci.* **2020**, *6*, 1401–1411.

(8) Su, L.; Mosquera, J.; Mabesoone, M. F. J.; Schoenmakers, S. M. C.; Muller, C.; Vleugels, M. E. J.; Dhiman, S.; Wijker, S.; Palmans, A. R. A., Meijer, E. W. Dilution-induced gel-sol-gel-sol transitions by competitive supramolecular pathways in water. *Science* **2022**, *377*, 213–218.

(9) Collin, D.; Viswanatha-Pillai, G.; Vargas Jentzsch, A.; Gavat, O.; Moulin, E.; Giuseppone, N., Guenet, J. M. Some Remarkable Rheological and Conducting Properties of Hybrid PVC Thermoreversible Gels/Organogels. *Gels* **2022**, *8*, 557.

(10) Dong, S.; Leng, J.; Feng, Y.; Liu, M.; Stackhouse, C. J.; Schonhals, A.; Chiappisi, L.; Gao, L.; Chen, W.; Shang, J.; Jin, L.; Qi, Z., Schalley, C. A. Structural water as an essential comonomer in supramolecular polymerization. *Sci. Adv.* **2017**, *3*, eaao0900.

(11) Zhang, Q.; Li, T.; Duan, A.; Dong, S.; Zhao, W., Stang, P. J. Formation of a Supramolecular Polymeric Adhesive via Water-Participant Hydrogen Bond Formation. *J. Am. Chem. Soc.* **2019**, *141*, 8058–8063.

(12) Bellot, M., Bouteiller, L. Thermodynamic description of bis-urea self-assembly: competition between two supramolecular polymers. *Langmuir* **2008**, *24*, 14176–14182.

(13) Ayzac, V.; Sallembien, Q.; Raynal, M.; Isare, B.; Jestin, J., Bouteiller, L. A Competing Hydrogen Bonding Pattern to Yield a Thermo-Thickening Supramolecular Polymer. *Angew. Chem., Int. Ed.* **2019**, *131*, 13987–13991.

(14) Ayzac, V.; Dirany, M.; Raynal, M.; Isare, B., Bouteiller, L. Energetics of Competing Chiral Supramolecular Polymers. *Chem. Eur. J.* **2021**, *27*, 9627–9633.

(15) Burger, N. A.; Pembouong, G.; Bouteiller, L.; Vlassopoulos, D., Loppinet, B. Complete Dynamic Phase Diagram of a Supramolecular Polymer. *Macromolecules* **2022**, *55*, 2609-2614.

(16) Burger, N. A.; Meier, G.; Bouteiller, L.; Loppinet, B., Vlassopoulos, D. Dynamics and Rheology of Supramolecular Assemblies at Elevated Pressures. *J. Phys. Chem. B* **2022**, *126*, 6713–6724.

(17) Vereroudakis, E., Vlassopoulos, D. Tunable dynamic properties of hydrogen-bonded supramolecular assemblies in solution. *Prog. Polym. Sci.* **2021**, *112*, 101321.

(18) Adelizzi, B.; Van Zee, N. J.; de Windt, L. N. J.; Palmans, A. R. A., Meijer, E. W. Future of Supramolecular Copolymers Unveiled by Reflecting on Covalent Copolymerization. *J. Am. Chem. Soc.* **2019**, *141*, 6110–6121.

(19) Mabesoone, M. F. J.; Palmans, A. R. A., Meijer, E. W. Solute-Solvent Interactions in Modern Physical Organic Chemistry: Supramolecular Polymers as a Muse. *J. Am. Chem. Soc.* **2020**, *142*, 19781–19798.

(20) Christian, S. D.; Taha, A. A., Gash, B. W. Molecular complexes of water in organic solvents and in the vapour phase. *Q. Rev., Chem. Soc.* **1970**, *24*, 20–36.

(21) Wolfenden, R., Radzicka, A. On the Probability of Finding a Water Molecule in a Nonpolar Cavity. *Science* **1994**, *265*, 936–937.

(22) Kuzina, M. A.; Kartsev, D. D.; Stratonovich, A. V., Levkin, P. A. Organogels versus Hydrogels: Advantages, Challenges, and Applications. *Adv. Funct. Mater.* **2023**, *33*, 2301421.

(23) Van Zee, N. J.; Adelizzi, B.; Mabesoone, M. F. J.; Meng, X.; Aloi, A.; Zha, R. H.; Lutz, M.; Filot, I. A. W.; Palmans, A. R. A., Meijer, E. W. Potential enthalpic energy of water in oils exploited to control supramolecular structure. *Nature* **2018**, *558*, 100–103.

(24) Van Zee, N. J.; Mabesoone, M. F. J.; Adelizzi, B.; Palmans, A. R. A., Meijer, E. W. Biasing the Screw-Sense of Supramolecular Coassemblies Featuring Multiple Helical States. *J. Am. Chem. Soc.* **2020**, *142*, 20191–20200.

(25) Iseki, T.; Mabesoone, M. F. J.; Koenis, M. A. J.; Lamers, B. A. G.; Weyandt, E.; de Windt, L. N. J.; Buma, W. J.; Palmans, A. R. A., Meijer, E. W. Temperature-dependent modulation by biaryl-based monomers of the chain length and morphology of biphenyl-based supramolecular polymers. *Chem. Sci.* **2021**, *12*, 13001–13012.

(26) Lortie, F.; Boileau, S.; Bouteiller, L.; Chassenieux, C., Lauprêtre, F. Chain Stopper-Assisted Characterization of Supramolecular Polymers. *Macromolecules* **2005**, *38*, 5283–5287.

(27) Pinault, T.; Andrioletti, B., Bouteiller, L. Chain stopper engineering for hydrogen bonded supramolecular polymers. *Beilstein J. Org. Chem.* **2010**, *6*, 869–875.

(28) Francisco, K. R.; Dreiss, C. A.; Bouteiller, L., Sabadini, E. Tuning the viscoelastic properties of bis(urea)-based supramolecular polymer solutions by adding cosolutes. *Langmuir* **2012**, *28*, 14531–14539.

(29) Louhichi, A.; Jacob, A. R.; Bouteiller, L., Vlassopoulos, D. Humidity affects the viscoelastic properties of supramolecular living polymers. *J. Rheol.* **2017**, *61*, 1173–1182.

(30) de Windt, L. N. J.; Mabesoone, M. F. J.; Weyandt, E.; Meijer, E. W.; Palmans, A. R. A., Vantomme, G. How to Determine the Role of an Additive on the Length of Supramolecular Polymers? *Organic Materials* **2020**, *02*, 129–142.

(31) Simic, V.; Bouteiller, L., Jalabert, M. Highly cooperative formation of bis-urea based supramolecular polymers. *J. Am. Chem. Soc.* **2003**, *125*, 13148–13154.

(32) Bouteiller, L.; Colombani, O.; Lortie, F., Terech, P. Thickness transition of a rigid supramolecular polymer. *J. Am. Chem. Soc.* **2005**, *127*, 8893–8898.

(33) Ducouret, G.; Chassenieux, C.; Martins, S.; Lequeux, F., Bouteiller, L. Rheological characterisation of bis-urea based viscoelastic solutions in an apolar solvent. *J. Colloid Interface Sci.* **2007**, *310*, 624–629.

(34) Shikata, T.; Nishida, T.; Isare, B.; Linares, M.; Lazzaroni, R., Bouteiller, L. Structure and dynamics of a bisurea-based supramolecular polymer in n-dodecane. *J. Phys. Chem. B* **2008**, *112*, 8459–8465.

(35) Burger, N. A.; Mavromanolakis, A.; Meier, G.; Brocorens, P.; Lazzaroni, R.; Bouteiller, L.; Loppinet, B., Vlassopoulos, D. Stabilization of Supramolecular Polymer Phase at High Pressures. *ACS Macro Lett.* **2021**, *10*, 321–326.

(36) Cates, M. E. Reptation of living polymers: dynamics of entangled polymers in the presence of reversible chain-scission reactions. *Macromolecules* **1987**, *20*, 2289–2296.

(37) Vereroudakis, E.; Van Zee, N.; Meijer, E. W., Vlassopoulos, D. Repeated shear startup response of a supramolecular polymer. *J. Non-Newtonian Fluid Mech.* **2023**, *315*, 105021.

(38) Ferry, J. D. *Viscoelastic Properties of Polymers*; Wiley: New York, NY, 1980.

(39) Honerkamp, J., Weese, J. A nonlinear regularization method for the calculation of relaxation spectra. *Rheol. Acta* **1993**, *32*, 65–73.

(40) Meier, G., Kriegs, H. A high pressure cell for dynamic light scattering up to 2 kbars with conservation of plane of polarization. *Rev. Sci. Instrum.* **2008**, *79*, 013102.

(41) Meier, G.; Vavrin, R.; Kohlbrecher, J.; Buitenhuis, J.; Lettinga, M. P., Ratajczyk, M. SANS and dynamic light scattering to investigate the viscosity of toluene under high pressure up to 1800 bar. *Meas. Sci. Technol.* **2008**, *19*, 034017.

(42) Royall, C. P.; Poon, W. C. K., Weeks, E. R. In search of colloidal hard spheres. *Soft Matter* **2013**, *9*, 17–27.

(43) Furst, E. M., Squires, T. M. *Microrheology*; Oxford University Press: Oxford, 2017.

(44) Peterson, J. D., Cates, M. E. A full-chain tube-based constitutive model for living linear polymers. *J. Rheol.* **2020**, *64*, 1465–1496.

(45) Guenet, J.-M. Thermodynamics and Kinetic Aspects. In *Organogels*; Springer: 2016, pp 17–36. DOI: 10.1007/978-3-319-33178-2.

(46) Guenet, J.-M. Physical Aspects of Organogelation: A Point of View. *Gels* **2021**, *7*, 65.

(47) Cates, M. E., Candau, S. J. Statics and dynamics of worm-like surfactant micelles. *J. Phys.: Condens. Matter* **1990**, *2*, 6869–6892.

(48) Rubenstein, M., Colby, R. H. *Polymer Physics*; Oxford University Press: Oxford, 2003.

(49) Calabrese, M. A.; Rogers, S. A.; Porcar, L., Wagner, N. J. Understanding steady and dynamic shear banding in a model wormlike micellar solution. *J. Rheol.* **2016**, *60*, 1001–1017.

(50) Gaudino, D.; Costanzo, S.; Ianniruberto, G.; Grizzuti, N., Pasquino, R. Linear wormlike micelles behave similarly to entangled linear polymers in fast shear flows. *J. Rheol.* **2020**, *64*, 879–888.

(51) Sato, T.; Moghadam, S.; Tan, G., Larson, R. G. A slip-spring simulation model for predicting linear and nonlinear rheology of entangled wormlike micellar solutions. *J. Rheol.* **2020**, *64*, 1045–1061.

(52) Peterson, J. D., Cates, M. E. Constitutive models for well-entangled living polymers beyond the fast-breaking limit. *J. Rheol.* **2021**, *65*, 633–662.

(53) *CRC Handbook of Chemistry and Physics, 90th Edition (CD-ROM Version 2010)*; Lide, D. R., Ed.; CRC Press/Taylor and Francis: Boca Raton, FL, 2010.

(54) Schmidt, R.; Schmutz, M.; Michel, M.; Decher, G., Mésini, P. J. Organogelation Properties of a Series of Oligoamides. *Langmuir* **2002**, *18*, 5668–5672.

(55) Lescanne, M.; Colin, A.; Mondain-Monval, O.; Fages, F., Pozzo, J. L. Structural Aspects of the Gelation Process Observed with Low Molecular Mass Organogelators. *Langmuir* **2003**, *19*, 2013–2020.

(56) Lescanne, M.; Grondin, P.; d'Aleo, A.; Fages, F.; Pozzo, J. L.; Monval, O. M.; Reinheimer, P., Colin, A. Thixotropic organogels based on a simple N-hydroxyalkyl amide: rheological and aging properties. *Langmuir* **2004**, *20*, 3032–3041.

(57) Riddick, J. A.; Bunger, W. B., Sakano, T. K. *Organic Solvents, Physical Properties and Methods of Purification*; John Wiley & Sons, 1986.

(58) Ortony, J. H.; Qiao, B.; Newcomb, C. J.; Keller, T. J.; Palmer, L. C.; Deiss-Yehiely, E.; Olvera de la Cruz, M.; Han, S., Stupp, S. I. Water dynamics from the surface to the interior of a supramolecular nanostructure. *J. Am. Chem. Soc.* **2017**, *139*, 8915–8921.

(59) Massiera, G.; Ramos, L., Ligoure, C. Role of the size distribution in the elasticity of entangled living polymer solutions. *Europhys. Lett.* **2002**, *57*, 127–133.

(60) Nakaya–Yaegashi, K.; Ramos, L.; Tabuteau, H., Ligoure, C. Linear viscoelasticity of entangled wormlike micelles bridged by telechelic polymers: An experimental model for a double transient network. *J. Rheol.* **2008**, *52*, 359–377.

(61) Zou, W.; Tan, G.; Jiang, H.; Vogtt, K.; Weaver, M.; Koenig, P.; Beaucage, G., Larson, R. G. From well-entangled to partially-entangled wormlike micelles. *Soft Matter* **2019**, *15*, 642–655.

(62) Cates, M. E. Dynamics of living polymers and flexible surfactant micelles : scaling laws for dilution. *J. Physique* **1988**, *49*, 1593–1600.

(63) Cates, M. E., Fielding, S. M. Rheology of giant micelles. *Adv. Phys.* **2006**, *55*, 799–879.

(64) Jansen, S. A. H.; Weyandt, E.; Aoki, T.; Akiyama, T.; Itoh, Y.; Vantomme, G.; Aida, T., Meijer, E. W. Simulating Assembly Landscapes for Comprehensive Understanding of Supramolecular Polymer-Solvent Systems. *J. Am. Chem. Soc.* **2023**, *145*, 4231–4237.

(65) Discussion of paper by A. Louhichi, A. R. Jacob, L. Bouteiller and D. Vlassopoulos, entitled 'Humidity affects the viscoelastic properties of supramolecular living polymers'. *J. Rheol.* **2017**, *61*, 1183–1184.

(66) Granek, R. Dip in G"(ω) of Polymer Melts and Semidilute Solutions. *Langmuir* **2002**, *10*, 1627–1629.

(67) Tan, G.; Zou, W.; Weaver, M., Larson, R. G. Determining threadlike micelle lengths from rheometry. *J. Rheol.* **2021**, *65*, 59–71.

(68) Rehage, H., Hoffmann, H. Rheological properties of viscoelastic surfactant systems. *J. Phys. Chem.* **1988**, *92*, 4712–4719.